Progress on the development of the Stellar X-ray Polarimeter on board of the Spectrum-X-Gamma Satellite (*)

P. SOFFITTA (1), L. BARBANERA (1), E. COSTA (1), G. DI PERSIO (1), M. FEROCI (1)
B. MARTINO (1), G. MATT (1)(**), L. PIRO (1), A. RUBINI (1), A. SANTANGELO (2)
S. GIARRUSSO (2), G. MANZO (2)(***), G. C. PEROLA (3), J. DWYER (4)(*$_*$*)
E. FORD (4), P. KAARET (4), R. NOVICK (4), R. ELSNER (5), M. WEISSKOPF (5)
E. SILVER (6), K. ZIOCK (6), I. LAPSHOV (7) and R. SUNYAEV (7)

(1) *IAS/CNR - Frascati (Roma), Italy*
(2) *IFCAI/CNR - Palermo, Italy*
(3) *III Università di Roma - Roma, Italy*
(4) *Columbia University, Physics Department - New York, NY, USA*
(5) *NASA/Marshall Space Flight Center - Huntsville, AL, USA*
(6) *Lawrence Livermore Laboratories - Livermore, CA, USA*
(7) *Space Research Institute of the Russian Academy of Science - Moscow, Russia*

(ricevuto il 5 Dicembre 1996; approvato il 18 Marzo 1997)

Summary. — We present the status of the Stellar X-ray Polarimeter at November '94 devoted to measure linear polarisation from cosmic X-ray sources between 2 keV and 15 keV which will be flown on the Spectrum-X-Gamma Satellite. In particular, we focus on the performances of the engineering model after the calibrations at Lawrence Livermore Laboratories and on the improvements which have been introduced on the four flight model imaging proportional counters which are key parts of the experiment.

PACS 98.70.Qy – X-ray sources.
PACS 95.55.Qf – Photometric, polarimetric, and spectroscopic instrumentation.
PACS 01.30.Cc – Conference proceedings.

1. – Introduction

X-rays produced by celestial sources can be polarised whenever the radiation is transported through non-spherically symmetric environment, such as in accretion disk

(*) Paper presented at the VII Cosmic Physics National Conference, Rimini, October 26-28, 1994.
(**) Now at III Università di Roma.
(***) Now at Istituto TESRE/CNR, Bologna.
(*$_*$*) Now at University of Maryland, USA.

on compact objects or whenever the radiation is produced in strong magnetic field. Even if the maximum degree of polarisation obtainable can be close to 100 % such as in cyclotron: line emission, many phenomena can contribute to lower this value. The Stellar X-ray Polarimeter on board the Spectrum-X-Gamma mission is designed to perform measurements with a minimum sensitivity of 1% and an observing time of 10^5 s for sources as faint as 50 mCrab. The engineering model of the Stellar X-ray Polarimeter has been fully tested and calibrated and the flight model is, at the time this paper is written, under construction. We present here the results of testing and calibrating the engineering model detector and the SXRP engineering model experiment.

2. – The design

The experiment is designed to be mounted at the focus of the 8 m focal length SODART telescope of the Spectrum-X-Gamma Satellite in continuous rotation with respect to the optical axis of the telescope.

A graphite crystal reflects at 45° the X-ray radiation in a secondary focus within a

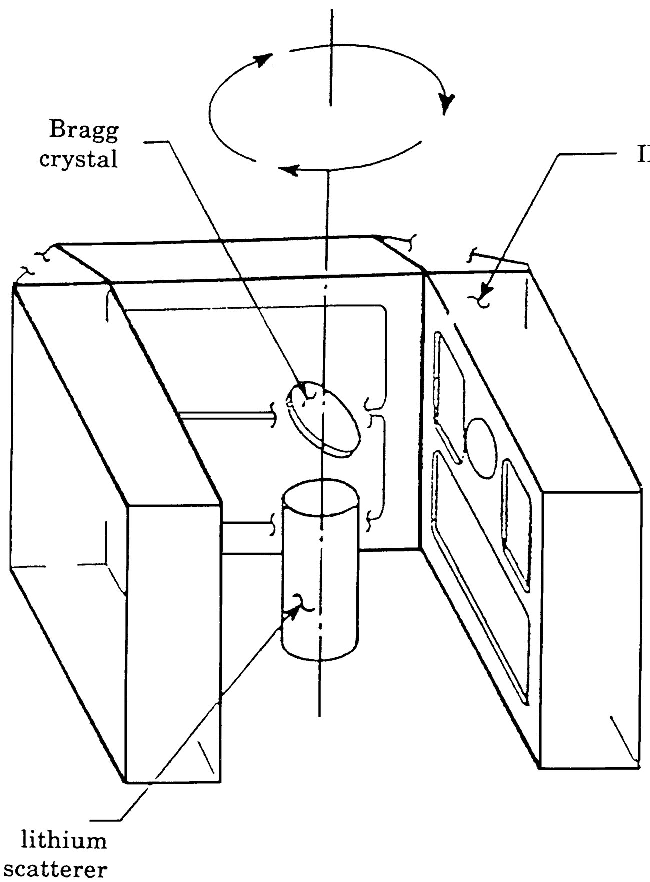

Fig. 1. – Sketch of the SXRP experiment on board the Spectrum-X-Gamma Satellite.

narrow band at 2.6 keV and 5.2 keV. The impinging radiation at higher energies is transmitted through the graphite crystal and it is diffused by a lithium rod onto four imaging proportional counters that surround the scatterer.

The detectors together with the lithium rod, the Bragg crystal and the high-voltage power supplies and the read-out electronics, are in continuos rotation with respect to the optical axis at a maximum speed of 1 turn/min. A sketch of the experiment is shown in fig. 1.

Once corrected for the systematic effect, the amplitude and the phase of the modulation curves are directly related to the amplitude and phase of the linear polarisation of the incoming X-ray photons.

3. – Calibration of the SXRP engineering model imaging proportional counter

The SXRP experiment is described in Kaaret *et al.* (1993). Hereafter we summarise the results of the calibration of the engineering model detectors and the variation of the flight model design we introduced that were based on these measurements.

It was foreseen that the two working IPCs, out of four for the flight model, were part of the engineering model SXRP experiment together with two dummy IPCs. One IPC devoted to detect only the 5–15 keV Thomson-diffused X-ray photons (HEIPC) and another IPC to detect the Bragg 2.6 keV and 5.2 keV diffracted and the Thomson-diffused X-ray photons (LEIPC), each of them integrated with 3 HVs power supply and one electronic box to read out six signals from the counter.

Each detector was tested in a beam line 3.2 m long by using an X-ray tube with a replaceable anode to get fluorescence lines from different material and a 255 pinholes mask placed on the detector window. While the tests at high energy were performed with the beamline in air, during the tests with the low-energy sources, the beamline was pumped down to less than 1 mTorr to increase the photon mean free path.

The gain of the detector was studied both by using a single X-ray source at different anode and cathode voltages and by varying the X-ray energy at a fixed anode gain. We operated the detectors at a maximum gain of $2 \cdot 10^4$ at the anode cathode effective voltage difference of 2240 V.

The position sensitivity of the detector is achieved by inserting a cathode plane made of aluminised kapton with a special pattern designed as wedges and strips. This method, first developed by Anger (1966), allows to detect the position of an X-ray interaction by using a linear combination of three signals. The typical distortions that appear on the pattern are due to the capacitance coupling between the wedge&strip cathode electrodes and the cross-talk between the electronic read-out. They can be easily removed, see fig. 2, when a mapping matrix is evaluated by best fit with the real positions of the pinholes.

We measured a position resolution of 1.5 mm at 5.9 keV at a gain of 10^4.

4. – Calibration of the whole SXRP engineering model

The sketch of the calibration chambers is shown in fig. 3.

On the left the SXRP chamber is shown in which the SXRP box is placed. A series of gimbals allow to dispose the SXRP axis with respect to the beam line axis to study both its response to known misalignments and reproducing the effect of the SODART

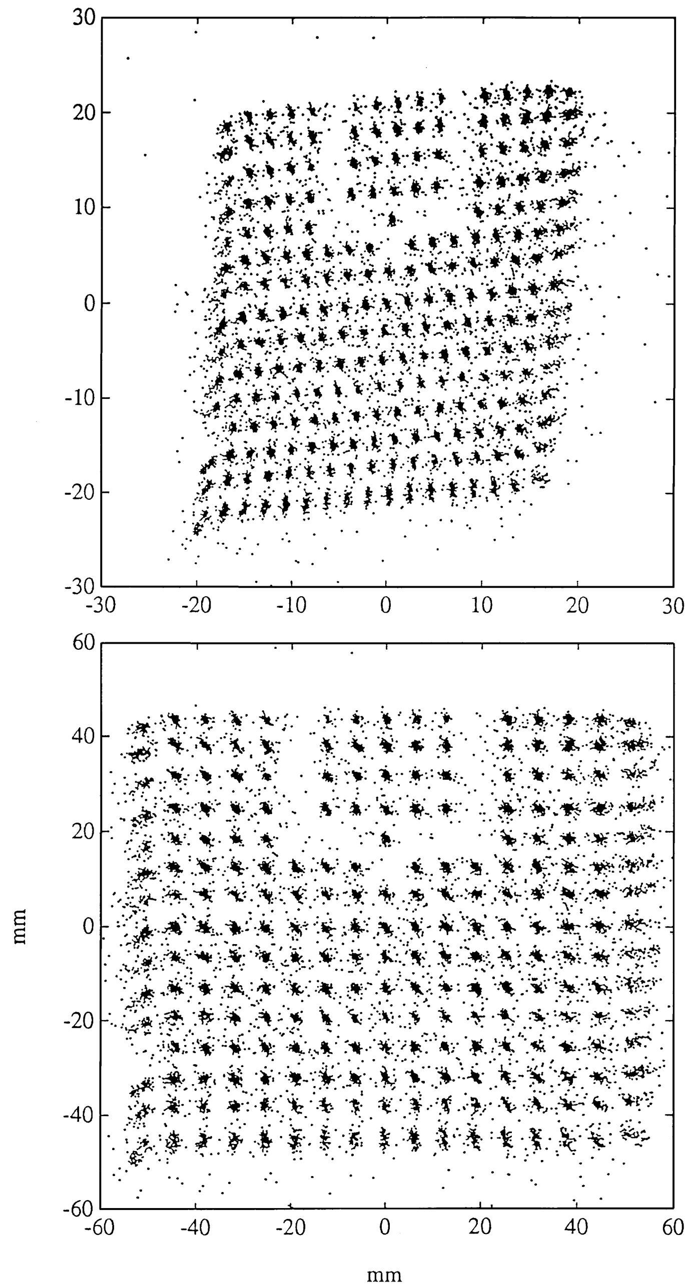

Fig. 2. – Positions of 255 pinholes illuminated by 9 keV X-ray source before (top) and after (bottom) applying the matrix deconvolution.

converging beam. A long tube connects the SXRP chamber to the source chamber and a valve allows to vent the source chamber without venting SXRP.

Two apertures, one in each chamber, define the X-ray axis for the measurement.

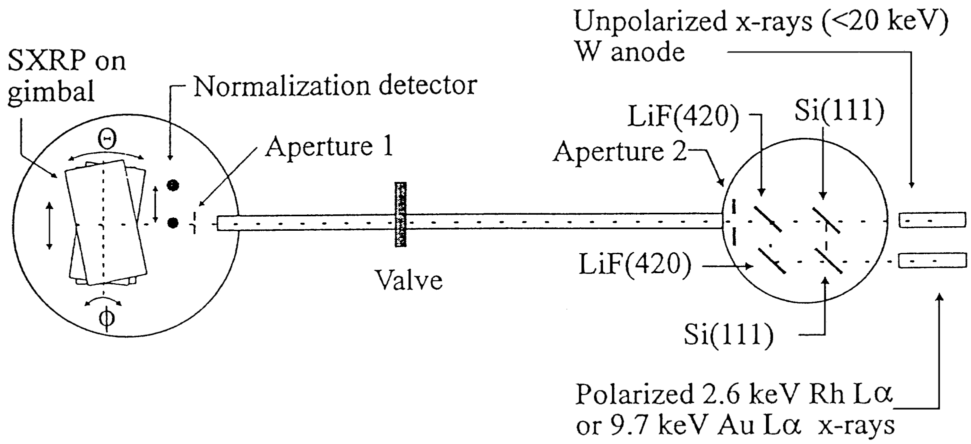

Fig. 3. – Sketch of the calibration chambers for the whole SXRP experiment.

The source chamber is designed to exchange three different X-ray generator tubes without requiring any new alignment. An X-ray generator tube with rhodium anode and another X-ray generator with gold anode were monochromatized and polarised close to 100% by using double diffraction on, respectively, Si (111) and on LiF (420) crystals. The unpolarised source was realised by using a W anode with a toroidal cathode to generate a continuum < 20 keV.

The SXRP worked by using a ground support equipment simulator with housekeeping readout. The acquisition of scientific data is continuously monitored.

Aim of the calibration is the measurement of the Modulation Factor of the Stellar X-ray Polarimeter: The sensitivity of a polarimeter is directly proportional to it. If we measure an azimuthal counting rate $N(\phi)$ we can decompose it in a Fourier series of the aximuthal angle ϕ:

$$N(\phi) = \sum_n a_n \cos[n(\phi - \phi_n)] .$$

In case of a 100% polarised X-ray source impinging on the polarimeter, and negligible background, the modulation factor μ is the amplitude of modulation for the second harmonic as:

$$\mu = a_2 / a_0 .$$

If the polarimeter rotates at an angular velocity ω, such component is often called 2ω component. For a partially polarised X-ray source, once known the modulation factor μ, the source counting rate r and the background counting rate b, the degree of polarisation can be evaluated as:

$$P = a_2 / a_0 (r + b) / \mu r .$$

The results are shown in fig. 4. We measured a modulation factor of 70% at 9.7 keV for the Thomson diffused photons. The amplitude of the modulation for the unpolarised on-axis source is 0.08% confirming the good control of the systematic effect. The 2ω for the Bragg-diffracted photons is 96%.

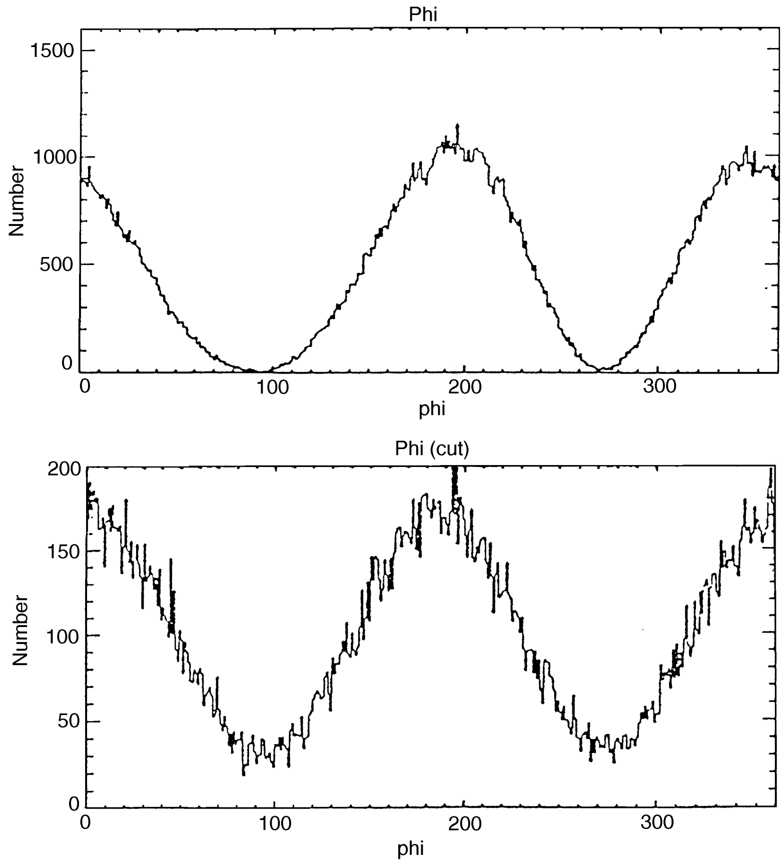

Fig. 4. – Response of the Bragg section (top) and Thomson section (bottom) at almost 100% polarized photons, respectively, of 2.69 keV and 9.7 keV. The amplitude of the modulation is 96% and 70%.

5. – **The flight model** IPCs

The calibration activity for the IPCs and the SXRP engineering model allowed to clarify some points that led us to make some change in designing and building the flight model detectors. All of this changes were in the direction of enhancing the survival capability of the detectors with the smallest impact possible on their performances taking into account the tight schedule of the experiment.

Actually, after the failure of the beryllium window during a vacuum cycling of one of the two engineering model detectors, we redesigned the support structure in a safer configuration by using titanium in place of the aluminium and by increasing the number of ribs. Other choices such as the use of curved beryllium window were strongly considered because of the lower shadowing of the support structure, but not implemented because of the schedule. The problem with the charge build-up on the dielectric substrate, already discussed in Soffitta *et al.* (1993), was solved by inserting a new cathode frame between the W&S plane and the antianode plane. The thin zero-field dead layer, does not decrease the performances on the background rejection of the anticoincidence region but prevent the ions from being collected on the kapton support foil of the W&S read-out system.

The sparking tests on the flight models revealed the weakness of the aluminisation substrate of the W&S read-out system. In some points the vaporisation of the aluminisation interrupted the connections. A safer cathode piane has been adopted by using electroformed copper in place of aluminium. The electroforming allows to grow a thicker metallic support capable of withstanding possible sparks. No evidence of copper line fluorescence was found in laboratory tests.

The engineering model mixture was 80% Xe, 10% Ar, 10% CH_4. The flight model detectors will use a gas mixture of 50% Xe, 40% Ar and 10% CH_4 at 1.2 bar of pressure. This choice was based either on the improved background rejection capability measured by lowering the fraction of xenon and on the consideration that a smaller amount of background counts in the SXRP energy is also expected with a smaller amount of xenon (Feroci *et al.* 1992).

A good percentage of xenon is anyway required to better exploit the sensitivity of the Thomson stage over 5 keV.

6. – Conclusions

After analysing the results of the engineering model detectors, we are confident that all the major problems connected with the developing of the SXRP experiment are solved and we expect to have SXRP flight model performed in a way suitable for having a big step forward in the knowledge of the polarisation of the X-rays by celestial source after two decades of silence.

Note added in proofs

This paper shows the status of the SXRP project at November '94. Nowadays many progresses have been made. The Flight Model of the SXRP experiment has been succesfully tested and then calibrated during summer '96 and it is ready to be shipped to Russia for the integration.

* * *

The SXRP experiment is the result of a co-operative effort of USA, UK, Russian and Italian institutions. The Italian participants acknowledge the financial support by Agenzia Spaziale Italiana. PS would also like to thank Mr. I. ROCHWARGER and Mr. H. DENNING of Columbia University together with Mr. H. SELTZER of Sandia National Laboratory and Mr. D. VAN LUE of Lawrence Livermore Laboratories.

REFERENCES

ANGER H. O., *Instrum. Soc. Am. Trans.,* **5** (1966) 311.

KAARET P., SCHWARTZ J., SOFFITTA P., DWYER J., SHAW P., HANANY S., NOVICK R., SUNYAEV R., LAPSHOV I., SILVER E., ZIOCK K. P., WEISSKOPP M. C., ELSNER R. F., RAMSEY B., COSTA E., RUBINI A., FEROCI M., PIRO L., MANZO G., GIARRUSSO S., SANTANGELO A., SCARSI L., PEROLA G. C., MASSARO E. and MATT G., *Proc. SPIE*, **2010** (1993) 22.

SOFFITTA P., BARBANERA L., COSTA E., DI PERSIO G., FEROCI M., MARTINO B., PIRO L., RUBINI A., MASSARO E., MEDICI G., PEROLA G. C., SANTANGELO A., GIARRUSSO S., LA ROSA G., MANZO G., FAZIO G., KAARET P., NOVICK R., LAPSHOV I. and SUNYAEV R., *Nuovo Cimento C,* **16** (1993) 703.

FEROCI M., COSTA E. and RAPISARDA M., *Proc. SPIE,* **1743** (1992) 104.